International Journal of Current Engineering and Technology
ISSN 2277 - 4106

Available at http://inpressco.com/category/ijcet

Research Article

Application of PNN for the Detection of QRS-complexes in Electrocardiogram using Combined Entropy

M. K. Bhaskar[a*], S. S. Mehta[a] , Guneet Singh Mehta[b] and N. S. Lingayat[c]

[a]Department of Electrical Engineering, M.B.M Engineering College, J.N.V University, Jodhpur, Rajasthan, India
[b]Department of Electrical Engineering, Indian Institute of Technology, Jodhpur, Rajasthan, India
[c]Department of Electrical Engineering, Dr. B.A.T. University, I.O.P.E., Lonere-402103, Maharashtra, India

Accepted 10 July 2013, Available online 01 August 2013, **Vol.3, No.3 (August 2013)**

Abstract

This paper presents a new classification scheme for the automatic detection of QRS-boundaries in Electrocardiogram (ECG) using Probabilistic Neural Networks (PNN). Digital filtering techniques are used to remove power line interference and baseline wander present in the ECG signal. PNN is used as a classifier to delineate QRS and non-QRS-regions in single-lead ECG signal. The algorithm is implemented using MATLAB. The performance of the algorithm is validated using each lead of the 12-lead simultaneously recorded ECGs from the dataset-3 of the CSE multi-lead measurement library. Significant detection rate of 99.50% is achieved. The percentage of false positive and false negative is 0.63% and 0.50% respectively. The overall results obtained show the capability of PNN in terms of the detection rate performance in comparison to the other methods reported in literature.

Keywords: *Delineation, Electrocardiogram (ECG), Morphologies of QRS-complexes, Probabilistic Neural Networks (PNN), QRS-complexes.*

1. Introduction

The Electrocardiogram (ECG) is the most useful and feasible diagnostic tool for initial evaluation, early risk stratification and triage. As displayed in Fig. 1, an ECG signal consists of a recurrent wave sequence of P-wave, QRS-complex and T-wave associated with each beat. Many cardiac abnormalities alter the heart's electrical activity and cause changes in the ECG. Since the electrical activity of both atria and ventricles is reflected in ECG, the test is of particular value in defining cardiac rhythms. Diseases which results in changes in the myocardial muscle mass will alter the ECG. For example, an increase in ventricular muscle mass (hypertrophy) usually results in larger QRS-amplitudes. Diseases which cause death of heart muscle and replacement by scar tissue (such as myocardial infractions) will be reflected in characteristic changes in morphology of the QRS-complex. Therefore, QRS-detection is an important step in almost all automated ECG analysis systems. The extensive review of the various methods developed for the detection of QRS-complexes is given in (B. U. Kohler*et al*, 2002; F. Gritzali,1988; O. Pahlm*et al*,1984; G. M. Friesen*et al*,1990). Few other QRS-detectors are reported recently using Hybrid Complex Wavelet (P. J. M. Fard*et al*,2007), transformative approach (M. B. Messaoud, 2007) , PCA-ICA based algorithm (M. P. S. Chawla,2007), continuous wavelet transform (A. Ghaffari, 2007), multiscale filtering based on mathematical morphology (F. Zhang*et al*,2007), Support Vector Machine (S. S. Mehta*et al*,2008) Adaptive quantized threshold (V. S. Chouhan*et al*,2008) etc. have been proposed. Most of the QRS-detectors consist of two main stages: a preprocessing stage, including linear filtering followed by nonlinear transformation and the decision rule. Digital filtering techniques are used in the present work to remove power line interference and baseline wander present in the ECG signal during preprocessing stage. PNN is used as a classifier to delineate QRS and non-QRS regions. Most of the QRS detection algorithms reported in literature detects R-peak locations and separate rules are applied for the delineation of QRS i.e. to locate the onsets and offsets of the QRS complexes. The proposed PNN based algorithm not only detects the QRS complexes but also delineates it simultaneously. The onsets and offsets of the detected QRS complexes are well within the tolerance limits specified by the expert cardiologists in the CSE study and are available in the CSE library.

Among many types of neural networks, the multilayer feed-forward neural network, also known as back propagation network, has become the main architecture of choice. One problem with this method is that back propagation is a stochastic searching algorithm to find the point with a minimum error in the error space. If the

*Corresponding author: M. K. Bhaskar

searching space is large, the training time becomes prohibitively long, without guaranteed global minimum. Another drawback of such architecture is that it is difficult to decide not only how many layers are needed but also how many neural nodes are required in each layer. All these parameters have to be tried experimentally, which is very time consuming. Furthermore, if the architecture of the neural network is decided after these tries and then fixed, the network will have difficulties to adapt itself to a new environment. To reduce these problems, Probabilistic Neural Networks (PNN) was proposed by Specht in 1988 and here in this proposed work PNN is applied as a classifier.

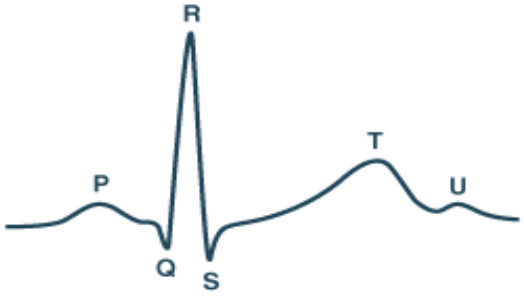

Fig.1 ECG signal

2. Probabilistic Neural Network

The Probabilistic Neural Network is a multilayered network. PNN provides a general solution to pattern classification problems. The basic idea behind PNN is the Bayes classification rule and Parzen's method of density estimation. The architecture and computation units of PNN implement these approaches. The most important advantage of PNN is that training is easy and instantaneous. Weights are not trained but assigned. Existing weights will never be altered but only new vectors are inserted into weight matrices during training. The PNN model of Mathwork's Matlab Neural Network Toolbox is used in the present work for the detection of QRS-complexes. The architecture of the PNN is shown in Fig. 2. The symbols and notations used in the Matlab Neural Network Toolbox are adopted in this section to describe the architecture of PNN. It has three layers: the input layer, the Radial Basis Layer and the competitive layer. Radial basis layer evaluates vector distances between input vector and row weight vectors in the weight matrix. These distances are scaled by Radial Basis Function non-linearly. Then the competitive layer finds the shortest distance among them, and thus finds the training pattern closest to the input pattern based on their distance.

The $R\times1$ dimensional input vector **p** is presented as a black vertical bar as shown in Fig. 2. In Radial Basis Layer, the vector distances between input vector **p** and the weight vector made of each row of the weight matrix **W** are calculated. The vector distance is defined as the dot product between the two vectors. Assuming the dimension of **W** as $Q\times R$, the dot product between **p** and the i^{th} row of **W** produces the i^{th} element of the distance vector $\| \mathbf{W} - \mathbf{p} \|$, whose dimension is $Q\times1$ as shown in Fig. 1. Then, the bias vector **b** is combined with $\| \mathbf{W} - \mathbf{p} \|$ by an element by element multiplication, represented as '.*' in Fig. 2 and the result is denoted as $\mathbf{n} = \| \mathbf{W} - \mathbf{p} \|.*\mathbf{b}$.

The transfer function in PNN has built into a distance criterion with respect to a center. It is defined as

$$radbas(n) = e^{-n^2} \quad (1)$$

Each element of **n** is substituted in Eq. (1) and produces corresponding element of **a**, the output vector of Radial Basis Layer. The i^{th} element of **a** can be represented as

$$a_i = radbas(\|\mathbf{W}_i - \mathbf{p}\|.*\mathbf{b}_i) \quad (2)$$

where $\mathbf{W}_i$ is the vector made of the i^{th} row of **W** and $\mathbf{b}_i$ is the i^{th} element of bias vector **b**.

The i^{th} element of **a** equals to 1 if the input **p** is identical to the i^{th} row of input weight matrix **W**. Radial basis neurons with a weight vector close to the input vector **p** produces a value near 1 and then its output weights in the competitive layer will pass their values to the competitive function. It is also possible that several elements of **a** are close to 1 since the input pattern is close to several training patterns.

***Q*=** number of input/target pairs = number of neurons in layer 1 and ***K*=** number of classes of input data = number of neurons in layer 2.

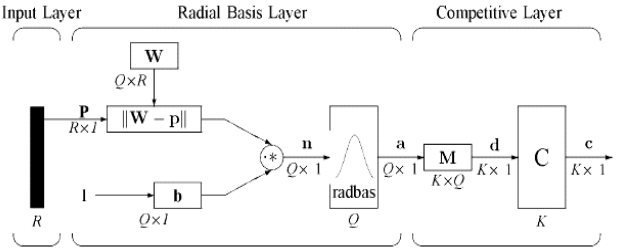

Fig. 2 : PNN Structure

There is no bias in a competitive layer. In this layer, the vector **a** is first multiplied with layer weight matrix **M**, producing an output vector **d**. The competitive function c, produces 1's corresponding to the largest element of **d** and 0's corresponding to the other elements. The output vector of the competitive function is denoted as **c**.

3. Pre-Processing of ECG Signal

A recorded ECG signal may contain noise from various sources. Therefore, before any kind of processing these noises should be minimized. This section describes the techniques used for the removal of power line interference, baseline wander and enhancement of the ECG signal. A raw ECG signal of a patient is acquired. The finite impulse response (FIR) notch filter proposed by Alste and Schilder (J. A. Van Alste*et al*,1985) is used to remove baseline wander. The adaptive filter to remove baseline wander is a special case of notch filter, with notch at zero frequency (or dc). This filter has a zero at dc and consequently creates a notch with a bandwidth of $(\mu/\pi)*f_s$, where f_s is the sampling frequency of the signal and μ is the

convergence parameter. Frequencies in the range 0-0.5 Hz are removed to reduce the baseline drift. The convergence parameter used is 0.0025. The filter proposed by Furno and Tompkins is used to remove 50Hz power line interference

The slope at every sampling instant of the filtered ECG signal is calculated and these are clustered into two classes, namely QRS-class and non-QRS-class using K-means of clustering algorithm (J. A. Van Alste*et al*,1985). Absolute slope is used as an important feature because absolute slope of the ECG signal is much more in the QRS-region than in the non-QRS-region. The probability, $P_i(x)$ of absolute slope at each sampling instant belonging to each of the two classes is calculated using (3).

$$P_i(x) = \frac{1}{\sqrt{2\pi}\sigma_i} \exp\left[-\frac{1}{2}\left(\frac{x - m_i}{\sigma_i}\right)^2\right]$$

$$i = 1, 2; \quad x = 1, 2, \ldots, s \qquad (3)$$

Where σ_i and m_i are the standard deviation and mean of i^{th} class and s represents total number of samples in the ECG signal.

Entropy is a statistical measure of uncertainty. A feature, which reduces the uncertainty of a given situation are considered more informative than those, which have opposite effect. Thus a meaningful feature selection criterion is to choose the features that minimize the entropy of the pattern class under consideration (J.L. Tou*et al*,1974).

The entropy $h_i(x)$ at each sampling instant for QRS and non-QRS-class is calculated using (4). These entropies are then normalized.

$$h_i(x) = -P_i(x)\log_e P_i(x), \qquad i = 1, 2; \; x = 1,2,\ldots, s \qquad (4)$$

The combined entropy, h_c is then calculated by using (5). Thereafter it is also normalized.

$$h_c(x) = (1 - h_{2n}(x)) * h_{1n}(x) \qquad (5)$$

Thus, from a single filtered ECG signal, one absolute slope curve; two normalized entropy curves, one from the QRS-entropies and other from the non-QRS-entropies; and one combined entropy curve are obtained. Similar procedure is applied for remaining leads of a subject and for all the subjects from the CSE ECG data-set 3.

Fig.3 shows the results of the preprocessing stage of lead II of record MO1_119 of the CSE ECG data-set 3. As depicted in Fig. 3(b), the preprocessor removes power line interference and baseline wander present in the raw ECG signal. The absolute slope of the ECG signal is much more in the QRS-region than in the non-QRS-region as displayed in Fig. 3(c). Fig. 3(d) shows $h_1(x)$, entropy curve for QRS-region. It can be seen from this curve that it has lower values in the QRS-region and higher values in the non-QRS-region. The low value of entropy in the QRS-region indicates lower uncertainty or in other words higher certainty of that region belonging to QRS-region. Similarly, higher values of entropy in the non-QRS-region indicate higher uncertainty or in other words lower certainty of that region belonging to QRS-region. Thus the entropy $h_1(x)$ curve provides critical information about the degree of certainty of a region belonging to QRS-region.

Fig. 3(e) shows $h_2(x)$, entropy curve for non-QRS-region. It can be seen from this curve that it has lower values in the non-QRS-region and higher values in the QRS-region. The low value of entropy in the non-QRS-region indicates lower uncertainty or in other words higher certainty of that region belonging to non-QRS-region. Similarly, higher values of entropy in the QRS-region indicate higher uncertainty or in other words lower certainty of that region belonging to non-QRS-region. Thus the entropy $h_2(x)$ curve provides critical information about the degree of certainty of a region belonging to non-QRS-region.

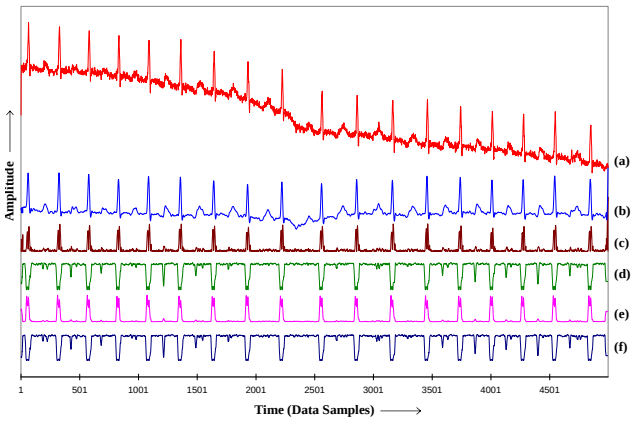

Fig.3 Results obtained at each step during preprocessing of the ECG Signal, (a) Raw ECG of record MO1_20 of CSE ECG database, (b) Filtered ECG Signal, (c) Entropy QRS (d) Entropy non-QRS, (e) [1- $h_{2n}(x)$] curve, (f) Combined Entropy.

The two entropy curves, $h_1(x)$ and $h_2(x)$, shown in Fig. 3(d) and (e) are normalized in order to obtain normalized entropy $h_{1n}(x)$ and $h_{2n}(x)$. Now if the curve, showing the product $h_c(x) = (1 - h_{2n}(x)) * h_{1n}(x)$ called combined entropy is obtained, it has much lower values in QRS-region and much higher values in non-QRS-region thus giving even better information as compared to $h_{1n}(x)$ and $h_{2n}(x)$ curves shown in Fig. 3(d) and (e). This can be seen in the combined entropy curve shown in Fig. 3(f). This makes the task of PNN classifier even easier for more reliable detection of QRS-complexes and drastic reduction in percentage of false positive and false negative detections as can be seen in the later part of this paper. In the present work, PNN algorithm is trained and tested separately using slope, entropy and combined entropy criteria for the detection of QRS-complexes in the single-lead and simultaneously recorded 12-lead ECG signal.

4. QRS-Detection Algorithm

The PNN model of Mathwork's Matlab Neural Network Toolbox is used for the detection of QRS-complexes. In this section a formal QRS detection algorithm is presented.

A. Step 1: Preprocessing of ECG Signal

1.1 Acquire raw ECG signal of a patient.
1.2 Use digital filtering techniques to remove baseline wander and power line interference.
1.3 Calculate the slope at every sampling instant of the filtered ECG signal.
1.4 Classify the slope values into two classes, namely QRS and non-QRS class using K-means of clustering algorithm.
1.5 Calculate the probability, $P_i(x)$ of slope at each sampling instant belonging to each of the two classes.
1.6 Calculate the entropy $h_i(x)$ at each sampling instant for QRS and non-QRS class to get two entropy curves.
1.7 Normalize these entropies.
1.8 Calculate the combined entropy $h_c(x)$

B. Step 2: Training of PNN

2.1 Select certain portions of ECGs covering a wide variety of QRS morphologies from the CSE dataset-3 to train PNN.
2.2 Transform the data to the format of PNN. Training instance matrix is an *R* by *Q* matrix of *Q* training instances. Where *R* = No. of elements in the input vector. In this case, the number of training instances is equal to the number of samples of the selected of ECGs covering a wide variety of QRS morphologies.
2.3 Select the value of spread, *s*. The value of *s* cannot be selected arbitrarily. A too small *s* value can result in a solution that does not generalize from the input/ target vectors used in the design. In contrast, if the spread constant is large enough, the radial basis neurons will output large values for all the inputs used to design a network. The optimum value of *s* obtained in the present work is 0.1.

C. Step 3: Testing of PNN

3.1 Begin with the first record of the CSE ECG dataset-3
3.2 Each record from CSE ECG data set 3 is of 10 second duration sampled at 500Hz, giving 5000 samples, i.e. 5000 testing instances.
3.3 For each testing instance, testing label of 1 is obtained if it belongs to the QRS region and a label of 0 is obtained if it belongs to the non-QRS region.

D. Step 4: Post processing phase

4.1 Club the continuous train of labels of 1's from the predicted labels to form a pulse of unit amplitude. Pick up the trains of labels of 1's and using their duration, calculate average pulse duration of 1's. Those trains of 1's, whose duration turns out to be more than the some fraction of average pulse duration, can be marked as QRS regions and the other ones as non-QRS regions.

4.2 In some cases, when the P or T waves are peaky in nature, the PNN gives trains of labels of 1's but of smaller duration as compare to that of QRS complex. In order to differentiate between trains of labels of 1's for QRS complex and peaky P or T waves, calculate an average duration of all the trains of labels of 1's. Those trains of labels of 1's whose duration is greater than some fraction of average pulse duration can be picked up as QRS complexes and others are discarded. Thus, average pulse duration criterion reduces the number of false positive detections.

5. Performance Evaluation

Dataset-3 of the CSE multi-lead measurement library (D. F. Specht,1988) is used for the performance evaluation of the proposed algorithm for QRS-detection. Detection is said to be true positive (TP) if the algorithm correctly identifies the QRS-complex and it is said to be false negative (FN) if the algorithm fails to detect the QRS-complex. False positive (FP) detections are obtained if non-QRS-wave is detected

TABLE-1 : Lead-wise detection of the QRS-complexes (Combined Entropy as Feature)

Lead	Total QRS	Correct Detection	False Positive	False Negative	% Detection
I	1488	1477	1	11	99.26
II	1488	1483	10	5	99.66
III	1488	1480	14	8	99.46
aVR	1488	1485	2	11	99.26
aVL	1488	1481	12	7	99.53
aVF	1488	1474	20	14	99.06
V1	1488	1485	9	3	99.80
V2	1488	1482	8	6	99.60
V3	1488	1479	16	9	99.40
V4	1488	1483	12	5	99.66
V5	1488	1481	2	7	99.53
V6	1488	1485	7	4	99.73
Total	**17856**	**17775**	**113 (0.63%)**	**90 (0.50%)**	**99.50**

as a QRS-complex. Detection rate of 99.50% is obtained when tested on 1500, single lead ECG recordings from the dataset-3. The lead-wise results of the QRS-detection are given in Table-1. The false positive detections are more in leads II, III, aVF, V3, V4 and V6 and very less in the remaining leads. Similarly, false negative detections are more in the leads I-III, and V3 and very low in the remaining leads. The percentage of false positive and false negative is 0.63% and 0.50% respectively. The proposed algorithm is capable for the detection all kind of morphologies of the QRS-complexes. QRS-detection in

the following figures demonstrates the strength of the proposed algorithm.

Table-2 : Lead-wise detection of the QRS-complexes

Sr. No.	Reference	Method	Number of Cases/beats used for testing	Detection rate
1	Proposed Algorithm (Combined Entropy as Feature)	Probabilistic Neural Network	125 cases, 17856 beats	99.50%
2	Mehta and Lingayat	Support vector machine	125 cases, 17856 beats	99.30%
3	Chouhan and Mehta	Adaptive quantized threshold	125 cases, 17856 beats	98.56%
4	Mehta*et al*.	Pattern Recognition	100 cases	99.83%
5	Saxena*et al*.	Wavelet transform	125 cases	99.86%
6	Gritzali	Length and energy transformation	14292 beats	99.60%
7	Kyrkos*et al*.	Time recursive prediction technique	1181beat	99%
8	Trahanias, and Skordalalkis	Bottom up approach	14292 beats	98.49%
9	Trahanias	Mathematical morphology	14292 beats	99.38%
10	Vijaya*et al*.	Neural network	3657beats	98.96%

The performance comparison of the proposed algorithm with the earlier published QRS-detection algorithms tested on the same CSE database is given in comparison Table-2. The performance of the algorithm compares favorably with other QRS-detection algorithms tested using CSE database.

Fig. 4 showing the steps for QRS-detection algorithm using PNN and combined entropy as feature in lead-aVL of record MO1_030. A raw ECG signal acquired as shown in Fig. 4(a). Filtered ECG is obtained using filtering techniques as shown in Fig. 4(b). In the next step calculate the entropy of QRS-region of the filtered ECG shown in Fig. 4(c), From the QRS-entropy curve it can be seen that the entropy belonging to QRS-class is low i.e. uncertainty of the occurrence of QRS is low or in other words certainty of the occurrence of QRS-region is high. Similarly the non-QRS curve is obtained as shown in Fig. 4(d). It can be seen that in QRS-region entropy belonging to non-QRS is high i.e. uncertainty of the occurrence of non-QRS is high or in other words certainty of non-QRS is low. Fig. 4(e) shows the combined entropy curve. Fig. 4(f) shows detection of QRS-complexes by PNN using combined entropy. Fig. 4(f) shows total QRS-candidates identified by the PNN which are thirteen in number. Whereas these are only twelve QRS-complexes present in the ECG under consideration. This has happened because of peaky noise present after the seventh QRS-complex. Whose combine entropy is comparable with that of QRS-complexes. In order to discard this wrongly detected QRS-candidates. Post-processing is done.

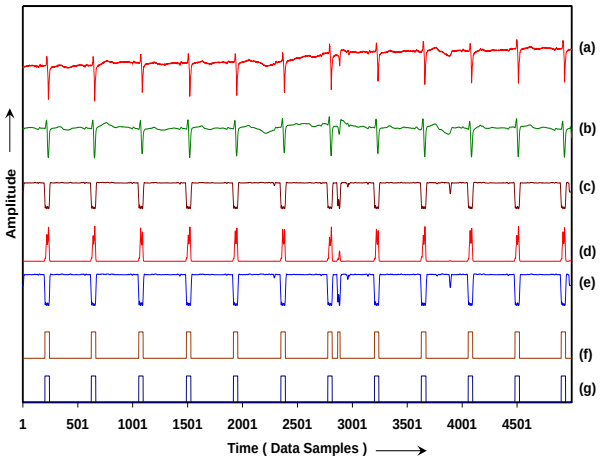

Fig. 4 : Steps for QRS-detection algorithm using PNN and Combined Entropy as feature in Lead-aVL of record MO1_030 (a) Raw ECG (b) Filtered ECG (c) Entropy QRS (d) Entropy Non-QRS (e) Combined Entropy (g) QRS-detection by PNN (h) QRS-detection by PNN after post-processing

The average pulse-width of all the QRS-candidates is calculated. Those QRS-candidates whose pulse-width turns out to be greater than average pulse-width are identified as true QRS-complexes. Whereas those, whose pulse-width turns out to be less than average pulse-width are discarded. Fig. 4(g) shows the QRS-complexes detected by PNN after post-processing, so therefore peaky noise has been dropped. Thus, with the help of post-processing the false positive cases are reduced and the accuracy of the algorithm is improved.

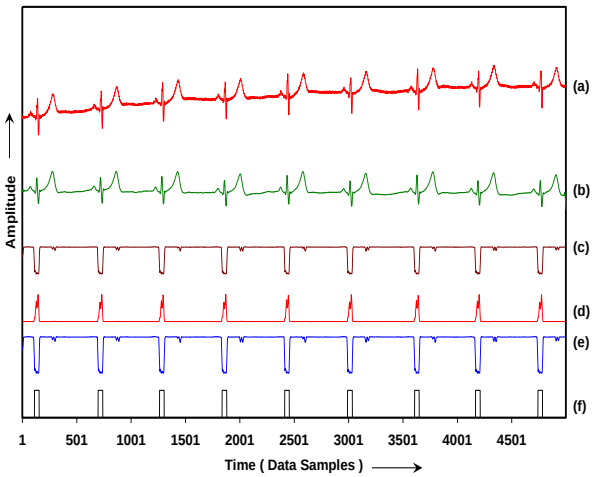

Fig. 5 : Detection of QRS using combined entropy as feature in Lead-II of record MO1_063 (a) Raw ECG (b) Filtered ECG (c) Entropy QRS (d) Entropy Non-QRS (e) Combined Entropy (f) QRS-detection by PNN

Fig.5 shows results obtained at the preprocessing stage and QRS-detection in lead-II of record MO1_063. As depicted in Fig. 5(b), the preprocessor removes noise and baseline wander present in the signal. The P-Waves are not prominent and T-waves are prominent in this case but their

combined entropies are very small as compared with that of QRS-complexes and hence they have been rightly not picked up as QRS-complex. It can be seen from Fig. 5(c) and (d) that in the QRS-region, the entropy belonging to QRS-class is low i.e. uncertainty of the occurrence of QRS is low or in other words certainty of the occurrence of QRS-region is high. Similarly, in this region entropy belonging to non-QRS is high i.e. uncertainty of the occurrence of non-QRS is high or in other words certainty of non-QRS is low. Since, the values of combined entropy is very low in QRS-region, hence all the QRS-complexes have been correctly identified by the PNN as shown in Fig. 5(f).

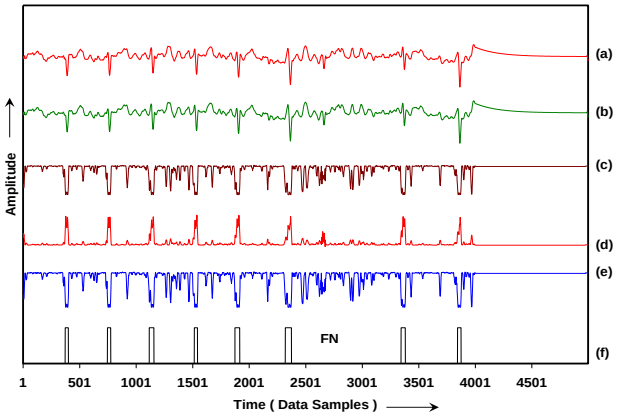

Fig. 6 : Detection of QRS using combined entropy as feature in Lead-aVF of record MO1_093 (a) Raw ECG (b) Filtered ECG (c) Entropy QRS (d) Entropy Non-QRS (e) Combined Entropy (f) QRS-detection

QRS-detection in lead-aVF of record MO1_093 is displayed in Fig. 6. The seventh QRS-complexes is not prominent in this case. As shown in Fig. 6(f), PNN fails to detect the seventh QRS-complex because of the higher value of QRS-entropy and lower value of non-QRS-entropies in the region of these QRS-complexes i.e. a case of false negative. While all other QRS-complexes having lower QRS-entropies and higher non-QRS-entropies have been successfully identified by the PNN.

6. Conclusion

The combined entropy criteria is very important in the process of QRS-detection because in this paper combined entropy is applied as feature signal. Much work has been carried out in the field of QRS-detection. Though the performance is good, each method has situations where it fails. Using the CSE database, the algorithm performed effectively with accurate QRS-detection over 99.50% of the total beats, even in the presence of peaky P and T-waves and wide variety of QRS-morphologies. The algorithm can be implemented more easily using PNN architecture of MATLAB to reproduce the results. The results shows that detection rate of QRS-complexes is quite encouraging.

References

B. U. Kohler, C. Henning, and R. Orglmeister (2002), The principles of software QRS detection, *IEEE Eng. in Med. and Bio*., vol. 21, pp. 42-47.

F. Gritzali (1988), Towards a generalized scheme for QRS Detection in ECG waveforms, in *Signal Processing*, vol. 15, pp. 183-192.

O. Pahlm and L. Sornmo (1984), Software QRS detection in ambulatory monitoring- A review, *Med. Biol. Eng. Comp.*, vol. 22, pp. 289-297.

G. M. Friesen, T. C. Jannett, M. A. Jadallah, S. L. Yates, S. R. Quint, and H. T. Nagle (1990), A Comparison of noise sensitivity of nine QRS detection algorithms, *IEEE trans on Biomed. Engg*., vol. 37, pp. 85-98.

P. J. M. Fard, M. H. Moradi, and M. R. Tajvidi (2007), A novel approach in R peak detection using Hybrid Complex Wavelet, *Int. J. Card*., doi:10.1016/j.ijcard.2006. 11.136.

M. B. Messaoud (2007), On the algorithm for QRS complex localization in Electrocardiogram, *I. J. of Computer Science and Network Security*, vol. 7, pp. 28-33.

M. P. S. Chawla, H. K. Verma, V. Kumar (2007), A new statistical PCA-ICA algorithm for location of R-peaks in ECG, *Int. J. Card*., doi: 10.1016/j.ijcard.2007.06. 036.

A. Ghaffari, H. Golbayni, and M. Ghasemi (2007), A new mathematical based QRS detectorsusing continous wavelet transform, *Computers and Electrical Engg*. doi:10.1016/j.compeleceng.2007.10.005

F. Zhang and Y. Lian (2007), Electrocardiogram QRS detectionusing multiscale filtering using wavelet transform, Proc. 29th Annual *Int. Conf. of the IEEE EMBS*, Lyon, France, pp. 3196-3199.

S. S. Mehta and N. S. Lingayat (2007), Development of Entropy based algorithm for cardiac beat detection in *12-lead electrocardiogram*, *Sig. Proc*., vol. 87, pp. 3190-3201.

S. S. Mehta and N. S. Lingayat (2008), Combined Entropy based method for detection of QRS complexes in 12-lead electrocardiogram using SVM, *Comp. in Biol. and Med*, vol. 38, pp. 138-145.

S. S. Mehta and N. S. Lingayat (2008), Detection of QRS Complexes in Electrocardiogram using Support Vector Machine, *Journal of Medical Engineering and Technology*, vol. 32, no. 3, pp. 206-215..

S. S. Mehta and N. S. Lingayat (2008), SVM-based algorithm for recognition of QRS complexes in Electrocardiogram, ITBM- RBM, doi:10.1016/ j.rbmret.2008.03.006

V. S. Chouhan and S. S. Mehta (2008), Detection of QRS-complexes in 12-lead ECG using adaptive quantized threshold, *IJCSNS International Journal of Computer Science and Network Security*, vol.8, no.1, pp. 155-163.

D. F. Specht (July 1988), Probabilistic neural networks for classification, mapping, or associative memory, Proc. *IEEE Int. Conf. Neural Networks, San Diego*, CA, vol. 1, pp. 525-532.

J. A. Van Alste, and T.S. Schilder (1985), Removal of base-line wander and power line interference from the ECG by an efficient FIR filter with a reduced number of taps, *IEEE Trans. Biomed. Eng*., vol. 32, pp.1052- 1059.

G. S. Furno, and W. J. Tompkins (1983), A learning filter for removing noise interference, *IEEE Trans. Biomed. Eng.*, vol. 30, pp. 234-235.

J.L. Tou and R.C. Gonzalez (1974), Pattern Recognition Principles, Addison-*Wesley Publishing Company* MA.

J. L. Willems, P. Arnaud, J. H. Van Bemmel, P. J. Bourdillon, R. Degani, B. Denis, I. Graham, F. M. A. Harms, P. W. Macfarlane, G. Mazzocca, J. Meyer, and C. Zywietz (1987), A

reference database for multilead electrocardiographic computer measurement programs, *J. Amer. Coll. Cardiol*., vol. 10, pp. 1313-1321.

S. S. Mehta, S.C. Sexana and H.K Verma (1996), Computer-aided interpretation of ECG for diagnostics, *Int. J. of System Science*, vol. 27, pp. 43-58.

S. C. Saxena, V. Kumar, S. T. Hamde (2002), Feature extraction from ECG signals using wavelet transform for disease diagnostics, *Int. J. of System Science*, vol . 33, pp. 1073- 1085.

F. Gritzali (1988), Towards a generalized scheme for QRS Detection in ECG waveforms, *Signal Processing*, vol.15, pp. 183-192, 1988.

A. Kyrkos, E. A. Giakoumakis, G. Carayannis (1988), QRS detection through time recursive prediction technique, *Signal Processing*, vol. 15, pp. 429-436.

P. Trahanias, E. Skordalalkis (1989), Bottom up approach to the ECG pattern-recognition problem, *Med. Bio. Eng. and Compu.*, vol . 27, pp. 221-229.

P. E. Trahanias (1993), An approach to QRS complex detection using mathematical morphology, *IEEE Trans. Biomed. Eng*., vol . 40, pp. 201-205.

Vijaya G, Kumar V, and Verma H. K. (0997), Artificial Neural Network Based Wave Complex Detection in Electrocardiograms, *Int. J. of System Science*, vol. 28,

Zahia Zidelmal, Ahmed Amirou, Mourad Adnane, Adel Belouchrani (2012), QRS detection based on wavelet coefficients, *Computer Methods and Programs in Biomedicine*,Volume 107, Issue 3, Pages 490-496.

Shih-Chin Fang, Hsiao-Lung Chan (April 2013), QRS detection-free electrocardiogram biometrics in the reconstructed phase space, *Pattern Recognition Letters*, Volume 34, Issue 5, 1 Pages 595-602.

C. Cros, M. Skinner, J. Moors, P. Lainee, J.P. Valentin (2012), Detecting drug-induced prolongation of the QRS-complex: New insights for cardiac safety assessment, *Toxicology and Applied Pharmacology*, Volume 265, Issue 2, Pages 200-208.

A. Ghaffari, M.R. Homaeinezhad, Y. Ahmadi (2010), An open-source applied simulation framework for performance evaluation of QRS-complex detectors, *Simulation Modelling Practice and* Theory, Volume 18, Issue 6, Pages 860-880

Takeshi Tsutsumi, Nami Takano, Narihisa Matsuyama, Yukei Higashi, Kuniaki Iwasawa, Toshiaki Nakajima (Oct 2011), High-frequency powers hidden within QRS-complex as an additional predictor of lethal ventricular arrhythmias to ventricular late potential in post–myocardial infarction patients, *Heart Rhythm*, Volume 8, Issue 10, Pages 1509-1515